STRAIN MEASUREMENTS AND DAMAGE DETECTION IN LARGE COMPOSITE STRUCTURES BY FIBER OPTICS SENSORS.

J. Sierra[a*], A. Güemes[b], M. Gómez[c]

[a]*Facultad de Ingeniería Aeronáutica, Grupo de Investigación en Ingeniería Aeroespacial, Universidad Pontificia Bolivariana, Medellín, Colombia*
[b]*Departamento de Materiales y Producción Aeroespacial, Universidad Politécnica de Madrid, Spain*
[c] *Simulación y Sistemas Logísticos, INDRA, Madrid, Spain*
** Julian.sierra@upb.edu.co*

Keywords: Strain field, Fiber Optic Sensors, Principal Component Analysis, Structural Health Monitoring, wind turbine blades.

Abstract

A 13.5 meters prototype of blade designed by Cener for a 150 kW wind turbine machine, made with glass fiber and vinylester resin doped with carbon nanofibers, was manufactured by Grupo Antolín using a new technique called Light RTM. The blade was done as a monocoque structure with a PVC foam core.

Indra and UPM have developed a methodology for instrumenting the blade with fiber optic sensors embedded into the structure during the manufacturing process. Two different sensing techniques were embedded into the blade: Fiber Bragg Gratings (FBG) and a plain fiber optic for Distributed Sensing using an Optical Backscatter Reflectometer (OBR).

By means of a novel and robust automated technique based in strain field pattern recognition, a study of detectability of defects was performed for the blade under different load scenarios. Several static tests were conducted, including a test campaign with known artificial damages induced into the structure and the sensitivity of the technique was evaluated. The results showed that every damages could be detected by using both sensing techniques.

1. Introduction

As the complexity of the structures increases, so do the physical and/or mathematical models that describe such structures as well as the techniques to ensure structural integrity during service life. At present various techniques for SHM (Structural Health Monitoring) for determining whether a structure is damaged at an early stage, are being developed by various research groups around the world. One of the proposed techniques is to detect subtle changes in the strain field by directly studying the correlations between different pairs of sensors. This technique is part of the philosophical SHM employing experimental data instead of deterministic models (such as the stiffness matrix, modal parameters, etc.). Experimental data are used for "training" or "learning" of different types of algorithms. The technique has been called "pattern recognition". Several authors have worked in recent years in the development of such techniques in order to predict the onset of damage in complex structures made of composite materials. In order to realize a dimensional reduction of the experimental data, and

filter useless or redundant data, a statistical technique called Principal Component Analysis (PCA) is adapted to pattern recognition. Nonlinear approximations like the Hierarchical Nonlinear PCA have been also applied in nonlinear problems [1], [2], [3], [4].

Regardless of the methodology used to analyze the data, the technique is based on a simple physical principle: the change in the local strain field and the local/global stiffness of a structure due to the occurrence of damage. Before applying different techniques of pattern recognition in a specific problem is important to consider whether the structure of interest, typical damages with similar severity to those expected during actual operation of the component, sufficiently alter the local strain field so that these changes are detectable with the proposed methodology. [3]

A simple form of such verification is to study the behavior of different pairs of sensors attached or embedded in the structure deformation. This technique has been called differential strains. Damage causes a change in the overall stiffness and, for different applied loads, a change in the local field distortion. Therefore, the relationship between the measured strains between two sensors in the presence of a change due to the change in the distribution of strains. [4].

The object of this study is to show the system implemented in which Fiber Bragg Gratings (FBGs) as strain sensors, directly embedded into the blade during manufacture are used to identify changes in the local/global stiffness of the structure, as consequence of the appearance of different types of damage induced in the blade. [5].

2. Principal Component Analysis

When performing experiments in the field of science, it is common to find a variety of systems in which the number of variables involved in the process can make the measurements become very complex. The main reason for this is that, in many cases, the relationships between variables may not be simple. An additional problem is how to represent the data when there are more than three variables since, visualize relationships between the different variables is more complex. Fortunately, in data samples where many variables are involved simultaneously, groups of variables often have similar trends as these groups may be "measuring" the same physical principle that governs the behavior of the system. In many physical systems, there are only a few "forces" that drive the system. When this happens, it is possible to take advantage of the redundancies, simplifying the problem by replacing a group of variables with a new single "virtual variable". [6]

PCA provides arguments on how to reduce complex data set to a smaller dimension and also reveals simpler patterns or "structures" that may be hidden under the data. The ultimate goal of the technique is to discern which data represent the most important dynamics of a particular system and which data, on the other hand, are redundant or just noise. This is achieved by determining a new coordinate space. This space is based on the covariance of the original data set.

In all experiments, measurements were done using several sensors (J), during certain time interval (K) and, for a discrete number of experimental trials (I). Then the information can be arranged in a tridimensional matrix (X_{3D}). In order to apply a PCA study, this matrix must be re-arranged in a proper way. This procedure is called 'unfolding'. The most common way of

unfolding when batch monitoring is desired, is the form $(I \times KJ)$, also called 'type D' unfolding. [7]

When different variables with different magnitudes and units are present in experiments, may be desirable to treat the data to reduce the 'scale effects', as this can hide important information about the system. The most usual way to do it is by normalizing the data. Normalization includes centering and scaling but is often called just 'scaling'. Centering deals with magnitude differences and scaling deals with differences in units. Several ways of normalizing information are reported on the literature.

Once the data matrix has been unfolded and normalized $(\bar{X})$ (if required), its covariance matrix is calculated. This square matrix measures the degree of linear relationships within the data set. The subspaces in PCA are defined by the eigenvalues and eigenvectors of the covariance matrix.

$$C_x P = P\Lambda \tag{1}$$

Where C_x is the covariance matrix, its associated eigenvectors are the columns of P, sorted in descendent order according to the value of their eigenvalues, which are the diagonal terms of Λ (these column vectors are called principal components). The projection of the original data over the direction of the principal components (P) is represented by the 'score matrix' (T) by the linear transformation given by:

$$T = \bar{X}P_r \tag{2}$$

Where P_r only contains the first r principal components.

In order to use PCA like a pattern recognition technique, a baseline must be built firstly, by using data for a known healthy structure. Then, data for unknown structure conditions should be projected into the baseline model (equation 2). From these projections it is possible to calculate different damage indices and detection thresholds.

Over the year, several variations, particularization and improvements to the PCA, have been developed in order to deal with specific problems. Perhaps, one of the most commons is the NLPCA, which allows to deal with nonlinear problems in a better way than linear PCA.

The NLPCA may be considered as a nonlinear generalization of the standard linear PCA. This generalization is achieved when the variables are projected onto surfaces or curves instead of planes or lines (like in PCA). [8]

As noticed by Scholz et al., NLPCA can be itself, subdivided in two different variations: normal NLPCA and h-NLPCA. The main difference between them is that h-NLPCA performs a dimensionality reduction by means of a hierarchical process. In this way, the data is decomposed in a PCA related way. The NLPCA is based on Multilayer Neural Networks.

In NLPCA, the mapping into feature space is generalized to allow arbitrary nonlinear functionalities. By analogous to the linear mapping performed by normal PCA, expressed in equation 2, NLPCA seeks for a mapping in the form:

$$T = f(\bar{X}(t)) \tag{3}$$

Where $f(\bar{X}(t))$ is a nonlinear vector function (projection function), composed of r individual nonlinear functions.

One of the most common statistical tools (also called 'damage indices') is the *Q* index, which indicates how well each sample fits the PCA model. The *Q* index is given by:

$$Q_i = \tilde{x}_i \tilde{x}_i^T = x_i (I - PP^T) x_i^T \quad (4)$$

3. Experimental setup

To conduct this experiment, a prototype of 13.5 m long of a wind turbine blade was used. The prototype was designed by CENER as part of the Spanish National project called NeWind. The prototype was manufactured by the company "Moldeo y Diseño". The UPM and INDRA worked together developing, manufacturing and testing a system to measure strains in wind turbine blades in real time and detect damages based on the strain measurements.

For the damage detection system four optical fibers were used, each one, having six FBGs. In total, 24 sensors were used. The sensors were located with a longitudinal separation of 2 m between them. Two optical fibers were located in the intrados and two in the extrados of the blade. The fibers were located at 20% and 80% of chord from the leading edge, along the span of the blade. The layout of the sensors network can be appreciated in detail in Figure 1. Besides the FBGs, it was decided to install four plain fiber optics at the surface of the blade to be interrogated with the OBR and, in this way, obtain distributed strain measurements during the tests. The plain optical fibers were installed in same positions than the FBGs.

The FBGs were interrogated with a Micron Optics SM130 and the plain optical fibers were interrogated with a LUNA OBR 4600. In order to multiplexing the OBR input, a LUNA FOS008 fiber optic switch 1 × 8 was used.

Once the blade was instrumented, it was attached to metal ring which allows to install the assembly in the test bench. It is important to notice that all tests were performed with the blade in cantilever. The load was applied in different points depending on the specific test. The main goal was trying to emulate the real load distribution. An automatic system of load application based on water deposits was used.

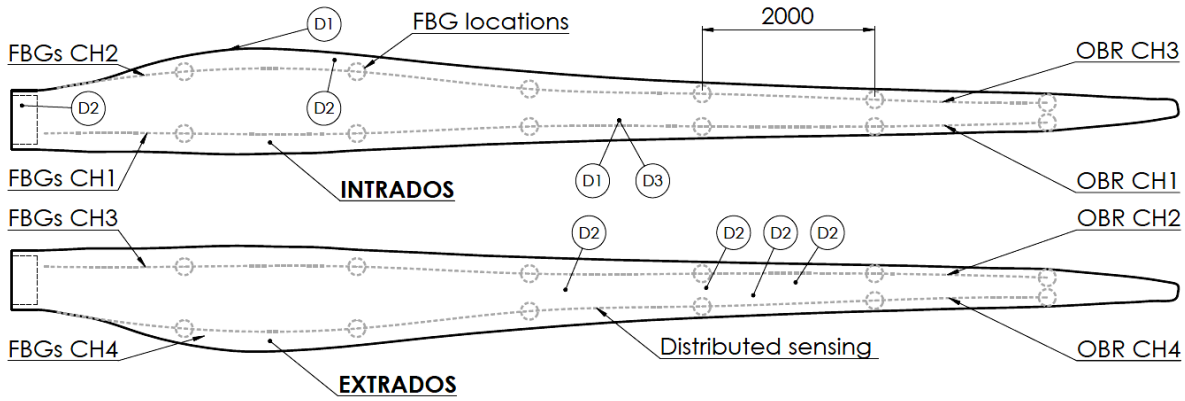

Figure 1. Sensors and damage locations. All units in mm.

The tests discussed in this article consisted in loading the blade in flapwise configuration (pressure side to suction side (PTS) or, the same, intrados to extrados). For the first test the blade was loaded up to 100% of the designed ultimate load. The procedure consisted in loading linearly until reaching a desired load level and, at this level, make a stop for measuring. The test started from 40% of the ultimate load. Each stop took 5 minutes, where all the measurements using the OBR were performed. For the first test, only stops were made at 50%, 60%, 70% and 100% of the ultimate load. The 80% and 90% stops were avoided fearing to damage the blade. The FBGs were interrogated during the duration of the whole experiments at a sampling rate of 5 Hz. Once reached the 100% of the ultimate load, the same procedure was repeated in order to unloading the blade. In both loading and unloading, OBR measurements were performed.

The second test, originally consisted in loading the blade to failure in PTS configuration. However, it was decided that, if the blade does not fail at 130% of the ultimate load, another test (third trial) will be performed. This time, an artificial damage will be induced in order to "compare" the damaged condition with the healthy one. Because this condition happened, it was possible to perform a study to compare the healthy structure against a damaged condition. The idea that the blade could reach 130% of the ultimate load was based in all the known uncertainties involved in the design and manufacturing of these prototypes, which involved new design methodologies, materials and manufacturing technologies.

The procedure was very similar to the procedure used for the first test. The load was increased linearly until, the desired load level was reached. Again, the starting point was chosen at 40% of the ultimate load. In this test, only stops were made at 70%, 80%, 90% and 100% of the ultimate load. It took three trials to break the blade. In the first one, the 130% of ultimate load was reached without any visible damage, then, as mentioned before, a third trial was performed, this time, inducing an artificial damage in the blade (D1). The first damage consisted in a cutting in the trailing edge, emulating a debonding. The cutting was located at 2.5 m from the root as it is shown in Figure 53. The damage has 10 cm length, 3 mm width and a depth of 3 cm. Additionally, a transversal cutting was made. This was located at the intrados skin, behind the cap, at 7 m from the root. This cutting has 13 cm length, 3 mm width and 13 mm depth.

During the loading stage in the third trial, there was an issue with the loading system when it reached 150% of the ultimate load and the test must be aborted. During the time in which the blade was loaded under 150% of ultimate load (more than 5 minutes), some visible damages (cracks) appeared in the surface of the blade in several positions. The exact locations of the cracks are presented in Figure 1. For this reason, the gathered data during loading stage was considered as one damage case (D1) and, the data gathered during unloading stage, was considered like a different damage case (D2, real damages).

In order to have a third damage case, before performing the fourth trial, another artificial damage was induced in the blade. The third damage consisted in increasing the size of the transversal cutting. Both, depths and width were increased to 30 mm and 15 mm respectively. Finally, in the third trial, the failure occurs around 186% of ultimate load.

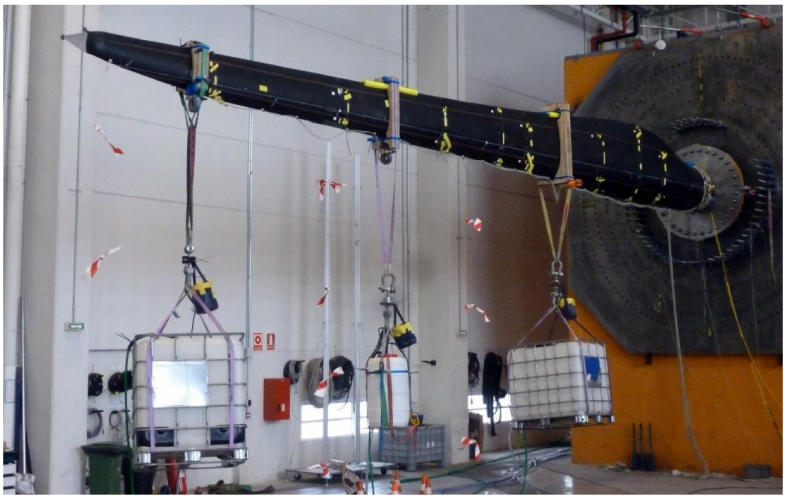

Figure 2. Experimental setup.

4. Results

All the experimental data matrices (unfolded and standarized) were "normalized" in order to have the same number of experimental measurements. Since all the experiment had different number of samples in function of time, for each one, one thousand points were took homogeneously distributed over the whole experiment (i.e. a modification of the sampling rate was performed in order to have the same amount of information for each experiment). This same procedure was used for the h-NLPCA study case.

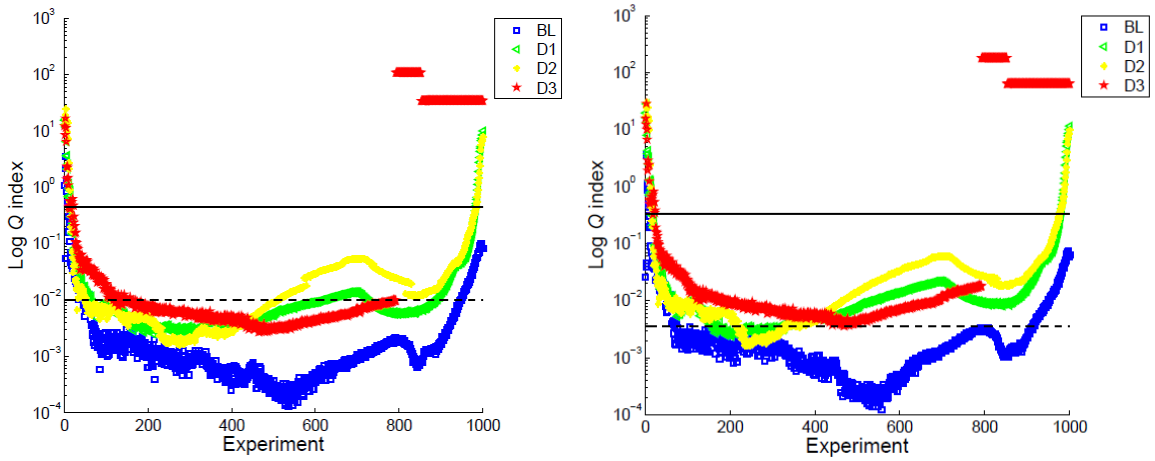

Figure 3. a) *Q* index for PCA model using the FBGs with damage thresholds for 95% and 99% of confidence (dashed line and solid line respectively). **b)** *Q* index for h-NLPCA model using the FBGs with damage thresholds for 95% and 99% of confidence (dashed line and solid line respectively).

For the Q index plot, presented in Figure 3 a), it is possible to see how the indices corresponding to the beginning and ending of the loading process lie outside the confidence intervals. These regions are more susceptible to nonlinearities since in that part of experiments, the strains start to distribute through the structure and the interaction between the blade and the fittings (brackets, load introduction system, etcetera) is stronger during this process. Besides this, the low SNR of the data in this region causes a loss in the sensitivity and therefore, some unusual phenomena like the indices out of the confidence interval close to beginning and ending of the experiment (lower load magnitudes near zero) as it can be seen.

As it can be seen in figure 3 b), there is a better fitting of the model. Almost all the baseline indices lie under the damage thresholds. However, there still remain some issues in the extremes of the experiment (lower load magnitudes), where some indices lie between the 95% and 99% of confidence. In this opportunity, the indices associated to the damaged conditions, in general terms, fall between the 95% and 99% of confidence intervals. This a better result than the obtained with the PCA model, since in this case, it would be possible to guarantee the damage apparition with 95% of confidence. Again, the indices corresponding to the massive failure (from sample 800 onwards for D3) lie far away from the baseline and obviously, can be classified as a clear damaged condition.

In this case, from the Q index point of view, it would not be possible to detect an abnormal condition clearly, with exception of the last samples for D3, which corresponds to the catastrophic failure of the blade and they are clearly out of all damage thresholds.

For the distributed sensing, 9646 sensors were defined for the four optical fibers. Only data for the loading stage of the load spectrum were used because for the OBR no data were acquire during the unloading process since it was carried out in a continuously way without stops.

In Figure 4 a) it is possible to appreciate how the indices corresponding to the damage cases lie outside the damage threshold. In this experiment by means of this index it would be possible to detect an abnormal condition clearly. There are a few outliers in the baseline which lie very close to the 99% threshold. However, it is not surprising since as mentioned in other sections, some spikes were found in some of the OBR measurements. These spikes were removed from data and some deviations from the baseline could be induced.

As can be seen in Figure 4 b), the results for the h-NLPCA model are very similar to those obtained with the PCA model. All the indices associated to the damaged states are well classified as abnormal conditions falling out the damage threshold. In this case the Q index is conclusive.

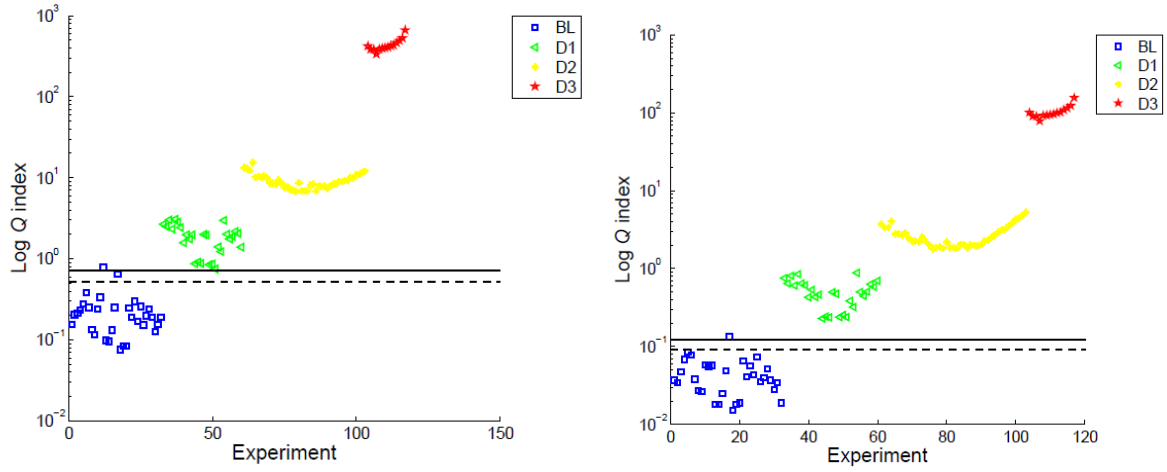

Figure 4. a) *Q* index for PCA model using the distributed sensing with damage thresholds for 95% and 99% of confidence (dashed line and solid line respectively). **b)** *Q* index for h-NLPCA model using the distributed sensing with damage thresholds for 95% and 99% of confidence (dashed line and solid line respectively).

5. Conclusions

Both PCA and h-NLPCA models were built by using strain measurements gathered from FBGs and distributed sensing. During subsequent steps, experiments were performed inducing three damages to the structure. All these experimental were projected into the PCA and h-NLPCA models and the *Q* index was calculated in order to achieve the first level of SHM. The effectiveness of the presented technique was tested using a real wind turbine blade 13.5 meters long fully made of composite material.

FBGs have shown to be very sensitive to small strain changes in the structure, which make them suitable for the proposed technique. However, in the dynamic case there are still issues to be solved to improve the technique. Distributed sensing shown to be more sensitive than discrete sensing because more sensors were used and OBR technique has higher resolution.

It was possible to detect deviations between the baseline and the different damage cases in all the presented examples. The Q index has shown to be very sensitive in this study.

Acknowledgements

The research included in this document was partially supported by the Spanish Ministry of Research through the project DPI2011-28033-C03-03

References

[1] L. Mujica, J. Rodellar, A. Fernandez and A. Guemes, Q-statistic and T2-statistic PCA-based measures for damage assessment in structures, *Structural Health Monitoring*, pp. 1-15, 2010.
[2] I. Lopez and N. Sarigul-Klijn, A review of uncertainty in flight vehicle structural damage monitoring, diagnosis and control: chalenges and opportunities, *Progress in aerospace sciences*, vol. 46, pp. 247-273, 2010.
[3] D. E. Adams, Health monitoring of structural materials and components, Lafayette: Jhon Wiley & Sons, 2007.
[4] J. Holnicki-Szulc, Smart technologies for safety engineering, Warsaw: Jhon Wiley & Sons, 2008.
[5] J. Sierra, A. Güemes and L. E. Mujica, Damage detection by using FBGs and strain field pattern recognition techniques, *Smart materials and structures*, vol. 22, pp. 1-10, 2013.
[6] R. Hajrya, N. Mechbal, and M. Verge, Damage detection of composite structure using independent component analysis, Conference on Control and Fault-Tolerant Systems, 2010
[7] P. Nomikos y J. F. MacGregor, Monitoring batch Processes Using Multiway Principal Component Analysis, *AIChE Journal* , pp. 1361-1375, 1994.
[8] M. Scholz and R. Vigário, Nonlinear PCA: a new hierachical approach, European Symposium on Artificial Neural Networks (ESSAN), 2002.